

Highlights from BESIII experiment

Hai-Bo Li¹ on behalf of the BESIII Collaboration
Institute of High Energy Physics
Beijing 100049, China

BESIII had collected large data samples on J/ψ and ψ' peaks during the first run in 2009. From 2010 to 2011, about 2.9 fb^{-1} integrated luminosity were obtained on the peak of $\psi(3770)$ for open charm physics. We review recent results on charmonium decays and hadron spectroscopy. The prospects on open charm physics are also discussed.

1 Introduction

The newly built BEPCII/BESIII is an upgrade to the previous BEPC/BES [1]. The BEPCII is a double ring collider with a design luminosity of $1 \times 10^{33} \text{ cm}^{-2} \text{ s}^{-1}$ at a center-of-mass energy of 3.78 GeV, which luminosity is one order of higher than that at CESR-c. It is operating between 2.0 and 4.6 GeV in the center of mass. The BESIII experiment is used to study the charm and τ physics. It is foreseen to collect on the order of 10 billion J/ψ events or 3 billion $\psi(2S)$ events per year according to the designed luminosity. About 32 million $D\bar{D}$ pairs and 2.0 million $D_S\bar{D}_S$ at threshold will be collected per year [1]. In last run, the peak luminosity of BEPCII has reached $6.4 \times 10^{32} \text{ cm}^{-2} \text{ s}^{-1}$.

The BESIII detector [1] consists of the following main components: 1) a main draft chamber (MDC) equipped with about 6500 signal wires and 23000 field wires arranged as small cells with 43 layers. The designed single wire resolution is $130 \mu\text{m}$ and the momentum resolution 0.5% at 1 GeV; 2) an electromagnetic calorimeter(EMC) made of 6240 CsI(Tl) crystals. The designed energy resolution is 2.5%@1.0 GeV and position resolution 6mm@1.0 GeV; 3) a particle identification system using Time-Of-Flight counters made of 2.4 m long plastic scintillators. The designed resolution is 80 ps for two layers, corresponding to a K/π separation (2σ level) up to 0.8 GeV; 4) a superconducting magnet with a field of 1 tesla; 5) a muon chamber system made of Resistive Plate Chambers(RPC).

In 2009, the BESIII had collected about 225 M and 106M data set on the J/ψ and ψ' peaks, respectively. About 2.9 fb^{-1} integrated luminosity on the $\psi(3770)$ peak had been accumulated for open charm physics, and the data size is about 3.5 times of that at CLEO-c. The results in this paper is based above data set.

¹lihb@ihep.ac.cn

2 Highlights from BESIII

The BESIII collaboration has published so-far a variety of papers with many new results in the field of light hadron and charmonium spectroscopy, as well as charmonium decays [2–11]. A number of new hadronic states were discovered or confirmed, and various decay properties were measured for the first time. In addition, many data analyses are in an advanced stage and will lead to a rich set of new publications in the near future. Here, we show recent highlights from the BESIII, thereby, illustrating the potential of the BESIII experiment. In this paper, for the reported experimental results, the first error and second error will be statistical and systematic, respectively, if they are not specified.

2.1 $\eta_c(1S)$ resonance via $\psi' \rightarrow \gamma\eta_c$ decay

Precise measurement of M1 transition of ψ' is important for us to understand the QCD in the relativistic and nonperturbative regimes. The $\psi' \rightarrow \gamma\eta_c$ transition is also a source of information on the η_c mass and width. There is currently a 3.3σ inconsistency in previous η_c mass measurements from J/ψ and $\psi' \rightarrow \gamma\eta_c$ (averaging $2977.3 \pm 1.3 \text{ MeV}/c^2$) compared to $\gamma\gamma$ or $p\bar{p}$ production (averaging $2982.6 \pm 1.0 \text{ MeV}/c^2$) [12]. The width measurements also spread from 15 to 30 MeV, it is around 10 MeV in the earlier days of experiments using J/ψ radiative transition [13, 14], while the recent experiments, including photon-photon fusion and B decays, gave higher mass and much wider width [15–18]. The most recent study by the CLEO-c experiment [19], using both ψ' and $J/\psi \rightarrow \gamma\eta_c$ decays, and pointed out there was a distortion of the η_c line shape. CLEO-c attributed the η_c line-shape distortion to the energy-dependence of the M1 transition matrix element. In the $J/\psi \rightarrow \gamma\eta_c$ from CLEO-c, the distorted η_c lineshape can be described by the relativistic Breit-Wigner (BW) distribution modified by a factor of E_γ^3 together with a dumping factor to suppress the tail on the higher photon energies. KEDR Collaboration did the same thing but tried different dumping factor [20].

Based on the data sample of 106 M ψ' events collected with BESIII detector, the η_c mass and width are measured from the radiative transition $\psi' \rightarrow \gamma\eta_c$. The η_c candidates are reconstructed from six exclusive decay modes: $K_s K\pi$, $K^+ K^- \pi^0$, $\eta \pi^+ \pi^-$, $K_s K^+ \pi^- \pi^+ \pi^-$, $K^+ K^- \pi^+ \pi^- \pi^0$, and $3(\pi^+ \pi^-)$, where K_s is reconstructed in $\pi^+ \pi^-$ mode, η and π^0 from $\gamma\gamma$ final states. For a hindered M1 transition the matrix element acquires terms proportional to E_γ^2 , which, when combined with the usual E_γ^3 term for the allowed transitions, lead to contributions in the radiative width proportional to E_γ^7 . Thus, the η_c lineshape is described by a BW modified by E_γ^7 convoluted with a resolution function. It is important to point out that the interference between η_c and non-resonance in the signal region is also considered. The statistical significance of the interference is 15σ . This affects the η_c resonant parameters significantly. Assuming an universal relative phase between the two amplitudes, we obtain η_c mass and width, $M = 2984.2 \pm 0.6 \pm 0.5 \text{ MeV}/c^2$ and $\Gamma = 31.4 \pm 1.2 \pm 0.6 \text{ MeV}$, respectively, as well as the relative phase $\phi = 2.41 \pm 0.06 \pm 0.04 \text{ rad}$. Figure 1 shows the

fit results in the six η_c decay modes. With precise measurement of the η_c mass, one can obtain the hyperfine splitting, $\Delta M_{hf}(1S)_{c\bar{c}} \equiv M(J/\psi) - M(\eta_c) = 112.5 \pm 0.8$ MeV, which agrees with the quark model prediction [21], and will be helpful for understanding the spin-dependent interactions in hidden quarkonium states.

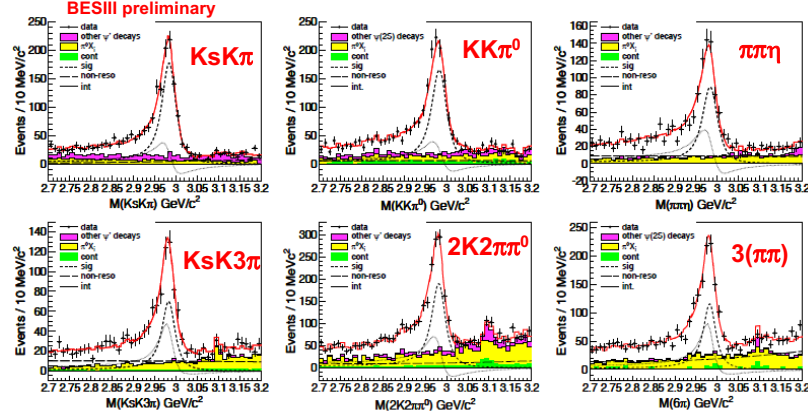


Figure 1: The invariant mass distributions for the decays $K_s K \pi$, $K^+ K^- \pi^0$, $\eta \pi^+ \pi^-$, $K_s K^+ \pi^- \pi^+ \pi^-$, $K^+ K^- \pi^+ \pi^- \pi^0$, and $3(\pi^+ \pi^-)$, respectively. Solid curves show the fitting results; the fitting components (η_c signal/non-resonance/interference) are shown as (dashed/long-dashed/dotted) curves. Points with error bar are data, shaded histograms are (in green/yellow/magenta) for (continuum/other η_c decays/other ψ' decays) backgrounds.

2.2 Observation of $\psi' \rightarrow \gamma \eta_c(2S)$

The first radially excited S-wave spin singlet state in the charmonium system, $\eta_c(2S)$, was observed by the Belle Collaboration in the decay process $B^\pm \rightarrow K^\pm \eta_c(2S)$, $\eta_c(2S) \rightarrow K_s K^\pm \pi^\mp$ [22]. It was confirmed by the CLEO [23] and BABAR [24] Collaborations in the two-photon fusion process $e^+ e^- \rightarrow e^+ e^- (\gamma \gamma)$, $\gamma \gamma \rightarrow \eta_c(2S) \rightarrow K_s K^\pm \pi^\mp$ and by the BABAR Collaboration in the double-charmonium production process $e^+ e^- \rightarrow J/\psi(c\bar{c})$ [25]. The only evidence for $\eta_c(2S)$ in the $\psi' \rightarrow \gamma \eta_c(2S)$ decay was from Crystal Ball Collaboration [26] by looking at the radiative photon spectrum. Recently, CLEO-c Collaboration searched for the $\psi' \rightarrow \gamma \eta_c(2S)$ signal with $\eta_c(2S)$ exclusive decay into 11 modes by using 25.9 M ψ' events, and no evidence found. Product branching fraction upper limits are determined as a function of $\Gamma(\eta_c(2S))$ for the 11 individual modes [27].

Using the largest ψ' data sample in the world which was collected by the BESIII, we searched for the M1 transition $\psi' \rightarrow \gamma \eta_c(2S)$ through the hadronic final states $K_s K^\pm \pi^\mp$. A bump is observed around 3635 MeV on the mass spectrum as shown in Fig. 2. In order to determine the background and mass resolution using data, the mass spectrum range is enlarged ($3.47 \sim 3.72$ GeV/ c^2) to include χ_{c1} and χ_{c2} events. The resonances χ_{c1} and χ_{c2}

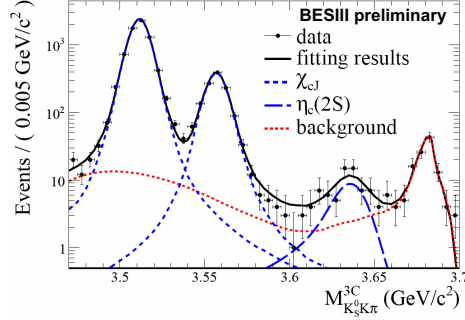


Figure 2: Fitting of the mass spectrum for $\eta_c(2S) \rightarrow K_s K^\pm \pi^\mp$.

are described by the corresponding Monte Carlo (MC) shape convolved a Gaussian which takes account the small difference on the mass shift and resolution between data and MC. So the mass resolution for the $\eta_c(2S)$ in the fitting is fixed to the linear extrapolation of the mass resolutions from the χ_{c1} and χ_{c2} signals in data. The line shape for $\eta_c(2S)$ produced by such the M1 transition is described by $(E_\gamma^3 \times BW(m) \times \text{damping}(E_\gamma)) \otimes \text{Gauss}(0, \sigma)$ where m is the invariant mass of $K_s K^\pm \pi^\mp$, $E_\gamma = \frac{m_{\psi'}^2 - m^2}{2m_{\psi'}}$ is the energy of the transition photon in the rest frame of ψ' , $\text{damping}(E_\gamma)$ is the function to damp the diverging tail raised by E_γ^3 and $\text{Gauss}(0, \sigma)$ is the Gaussian function describing the detector resolution. The possible form of the damping function is somewhat arbitrary, and one suitable function used by KEDR for a similar process is [20]

$$\frac{E_0^2}{E_\gamma E_0 + (E_\gamma E_0 - E_0)^2}$$

where $E_0 = \frac{m_{\psi'}^2 - m_{\eta_c(2S)}^2}{2m_{\psi'}}$ is the peaking energy of the transition photon. In the fit, the width of $\eta_c(2S)$ is fixed to PDG value. From the fit to the data, a signal with a statistical significance of 6.5 standard deviation is observed which is the first observation of the M1 transition $\psi' \rightarrow \gamma \eta_c(2S)$. The measured mass for $\eta_c(2S)$ is $3638.5 \pm 2.3 \pm 1.0 \text{ MeV}/c^2$. The measured branching ratio is $BR(\psi' \rightarrow \gamma \eta_c(2S)) \times BR(\eta_c(2S) \rightarrow K_s K^\pm \pi^\mp) = (2.98 \pm 0.57 \pm 0.48) \times 10^{-6}$. Together with the BABAR result $BR(\eta_c(2S) \rightarrow K \bar{K} \pi) = (1.9 \pm 0.4 \pm 1.1)\%$ [28], the M1 transition rate for $\psi' \rightarrow \gamma \eta_c(2S)$ is derived as $BR(\psi' \rightarrow \gamma \eta_c(2S)) = (4.7 \pm 0.9 \pm 3.0) \times 10^{-4}$.

Most recently, the Belle Collaboration measured $\eta_c(1S)$ and $\eta_c(2S)$ resonant parameters in the decay of $B^\pm \rightarrow K^\pm (K_s K \pi)^0$ by considering the interference between $\eta_c(1S)/\eta_c(2S)$ decay and non-resonant in the B^\pm decay [30]. Meanwhile, the BABAR Collaboration also updated the analysis of $e^+ e^- \rightarrow e^+ e^- (\gamma \gamma), \gamma \gamma \rightarrow \eta_c(1S)/\eta_c(2S) \rightarrow (K_s K \pi)^0$ and $K^+ K^- \pi^+ \pi^- \pi^0$ modes [31]. Table 1 shows the summary of the typical production processes (ψ' radiative decays, $\gamma \gamma$ fusion and B decays) for $\eta_c(1S)/\eta_c(2S)$ and corresponding resonant parameter measurements. These results indicate that the $\eta_c(1S)$ parameters agree well from

	BESIII [29] $\psi' \rightarrow \gamma\eta_c/\eta_c(2S)$	Belle [30] B decays	BABAR [31] $\gamma\gamma$ fusion	PDG 2010 [12]
$M(\eta_c(1S))$ MeV/ c^2	$2984.4 \pm 0.5 \pm 0.6$	$2985.4 \pm 1.5^{+0.2}_{-2.0}$	$2982.2 \pm 0.4 \pm 1.4$	2980.3 ± 1.2
$\Gamma(\eta_c(1S))$ MeV	$30.5 \pm 1.0 \pm 0.9$	$35.1 \pm 3.1^{+1.0}_{-1.6}$	$32.1 \pm 1.1 \pm 1.3$	28.6 ± 2.2
$M(\eta_c(2S))$ MeV/ c^2	$3638.5 \pm 2.3 \pm 1.0$	$3636.1^{+3.9+0.5}_{-1.5-2.0}$	$3638.5 \pm 1.5 \pm 0.8$	3637 ± 4
$\Gamma(\eta_c(2S))$ MeV	12 (fixed)	$6.6^{+8.4+2.6}_{-5.1-0.9}$	$13.4 \pm 4.6 \pm 3.2$	14 ± 7

Table 1: Comparison of the mass and width for $\eta_c(1S)/\eta_c(2S)$ in different production processes, $\psi' \rightarrow \gamma\eta_c(1S)/\eta_c(2S)$, $B^\pm \rightarrow K^\pm\eta_c(1S)/\eta_c(2S)$ and $\gamma\gamma$ fusion, from different experiments. The PDG values are only world average from earlier results. . For the time being, the most precise measurements for $\eta_c(1S)$ resonance are from BESIII, while these for $\eta_c(2S)$ resonant parameters are from BABAR in $\gamma\gamma$ fusion.

different production processes.

2.3 $h_c(1P)$ properties

The BESIII Collaboration reported the results on the production and decay of the h_c using 106M of ψ' decay events in 2010 [2], where we studied the distributions of mass recoiling against a detected π^0 to measure $\psi' \rightarrow \pi^0 h_c$ both inclusively (E1-untagged) and in events tagged as $h_c \rightarrow \gamma\eta_c$ (E1-tagged) by detection of the E1 transition photon. In 2011, 16 specific decay modes of η_c are used to reconstruct η_c candidates in the decay mode of $h_c \rightarrow \gamma\eta_c$. Figure 3 shows the π^0 recoiling mass for individual η_c decay modes in the decay chain of $\psi' \rightarrow \pi^0 h_c$, $h_c \rightarrow \gamma\eta_c$, while Fig. 4 is the sum of the 16 decay modes. We fit the 16 π^0 recoil-mass spectra simultaneously that yields $M(h_c) = 3525.31 \pm 0.11(stat.) \pm 0.15(syst.)$ MeV/ c^2 and $\Gamma(h_c) = 0.70 \pm 0.28(stat.) \pm 0.25(syst.)$ MeV/ c^2 . These preliminary results are consistent with the previous BESIII inclusive results and CLEO-c exclusive results.

The centroid of the 3P_J states ($\chi_{c0}, \chi_{c1}, \chi_{c2}$) is known to be $\langle M(^3P_J) \rangle = [5M(^3P_2) + 3M(^3P_1) + M(^3P_0)] = 3525.30 \pm 0.04$ MeV [12]. If the 3P_J states centroid mass $\langle M(^3P_J) \rangle$ is identified as the mass of $M(^3P)$, then BESIII observes the hyperfine splitting as $\Delta M_{hf}(1P)_{cc} = -0.01 \pm 0.11(stat.) \pm 0.14(syst.)$ MeV which agrees with zero.

We also look at the $\eta_c(1S)$ mass distributions in the exclusive decay modes. Figure 5 shows the distribution of invariant mass distribution from exclusive hadronic decays of $\eta_c(1S)$, the shape of the η_c is symmetric in $h_c(1P) \rightarrow \gamma\eta_c(1S)$ radiative transition and no distortion observed as in $J/\psi/\psi'$ radiative decays. The analysis is still on going for the resonant parameters.

2.4 The radiative decays $\psi' \rightarrow \gamma P$ with $P = \{\pi^0, \eta, \eta'\}$

The radiative decay of the ψ' to a pseudo-scalar meson, such as the π^0 , η , and η' , is of interest since it can be used to study the two-gluon coupling to $c\bar{c}$ states, to study the

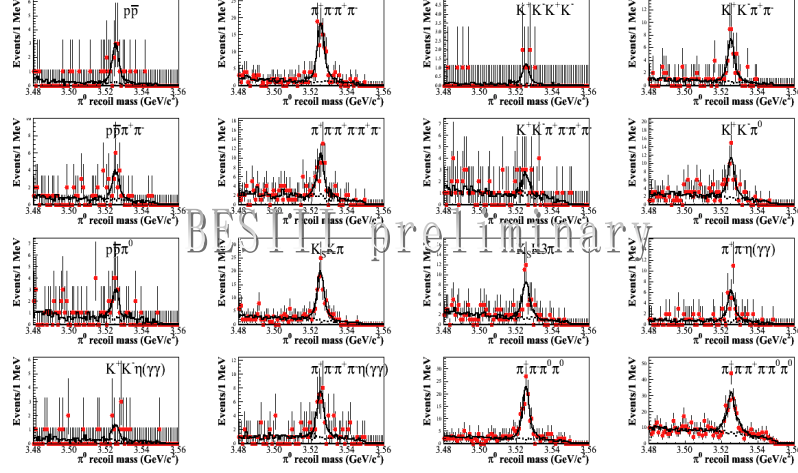


Figure 3: The π^0 recoiling mass for 16 η_c decay modes.

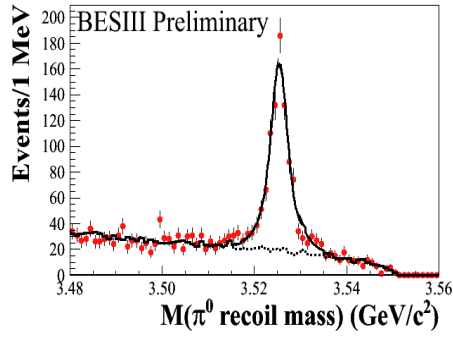


Figure 4: The π^0 recoiling mass for the sum of 16 η_c decay modes.

$\eta - \eta'$ mixing angle, and to probe the π^0 form factor in the time-like region. Recently, the CLEO-c Collaboration reported measurements for the decays of J/ψ , ψ' , and ψ'' to γP [32], and no evidence for $\psi' \rightarrow \gamma\eta$ or $\gamma\pi^0$ was found. With 106M ψ' data sample at BESIII, the processes $\psi' \rightarrow \gamma\pi^0$ and $\psi' \rightarrow \gamma\eta$ are observed for the first time with signal significances of 4.6σ and 4.3σ , respectively, and with branching fractions of $B(\psi' \rightarrow \gamma\pi^0) = (1.58 \pm 0.40 \pm 0.13) \times 10^{-6}$ and $B(\psi' \rightarrow \gamma\eta) = (1.38 \pm 0.48 \pm 0.09) \times 10^{-6}$. With a measured branching fraction, $B(\psi' \rightarrow \gamma\eta') = (126 \pm 3 \pm 8) \times 10^{-6}$. The mass distributions of the pseudo-scalar meson candidates can be found in Fig. 6 the BESIII Collaboration determined for the first time the ratio of the η and η' production rates from ψ' decays, $R_{\psi'} \equiv B(\psi' \rightarrow \gamma\eta)/B(\psi' \rightarrow \gamma\eta') = (1.10 \pm 0.38 \pm 0.07)\%$. This ratio is below the 90% C.L. upper bound determined by the CLEO-c Collaboration and, in contradiction to predictions of leading-order perturbative-QCD, one order of magnitude smaller than the corresponding ratio for the J/ψ decays, $R_{J/\psi} = (21.1 \pm 0.9)\%$. More details on the data analysis can be

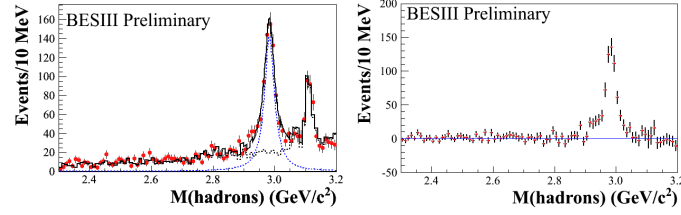


Figure 5: The invariant mass distributions for the sum of 16 η_c decay modes. Right is background subtracted.

found in Ref. [3]. These observations are interpreted in the framework of vector meson dominance (VMD) in association with the $\eta_c - \eta(\eta')$ mixings due to the axial gluonic anomaly [33].

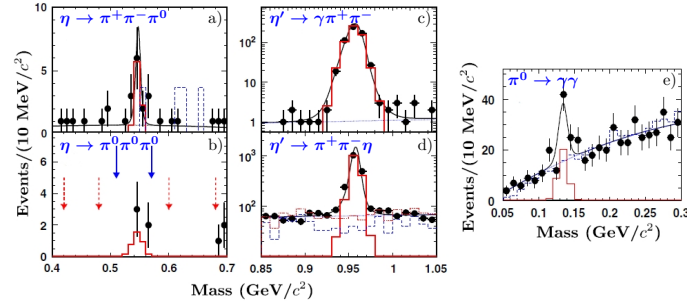


Figure 6: Mass distributions of the pseudo-scalar meson candidates for $\psi' \rightarrow \gamma P$: a) $P = \eta(\rightarrow \pi^+ \pi^- \pi^0)$; b) $P = \eta(\rightarrow 3\pi^0)$; c) $P = \eta'(\rightarrow \gamma \pi^+ \pi^-)$; d) $P = \eta'(\rightarrow \pi^+ \pi^- \eta(\rightarrow \gamma \gamma))$; e) $P = \pi^0(\rightarrow \gamma \gamma)$. For more details, we refer to Ref. [3].

2.5 Measurements of $J/\psi \rightarrow N\bar{N}$ branching fractions

The expected three main contributions to the decay $J/\psi \rightarrow N\bar{N}$ are shown in Fig. 7. This decay mode should be a very good test of PQCD, because of the 3 gluons in the OZI violating J/ψ strong decay just matching the 3 $(q\bar{q})$ pairs (as in Fig. 7(a)). The ratio between $BR(J/\psi \rightarrow n\bar{n})$ and $BR(J/\psi \rightarrow p\bar{p})$ strongly depends on the phase between the strong and the electromagnetic (e.m.) contributions as shown in Fig. 7 [34]. According to PDG values, $BR(J/\psi \rightarrow n\bar{n})$ is very similar to $BR(J/\psi \rightarrow p\bar{p})$, which gives a clear indication that strong and e.m. contributions do not interfere and have to be added in quadrature. An estimate for the relative phase ϕ on the basis of previous experimental results is $\phi = 89^\circ \pm 15^\circ$ [34]. However, the current experimental uncertainty on $BR(J/\psi \rightarrow n\bar{n})$ is still large $[(2.2 \pm 0.4) \times 10^{-3}]$, which is main contribution to the uncertainty on the phase determination. Therefore, it motivates the BESIII experiment to measure $J/\psi \rightarrow n\bar{n}$ decay

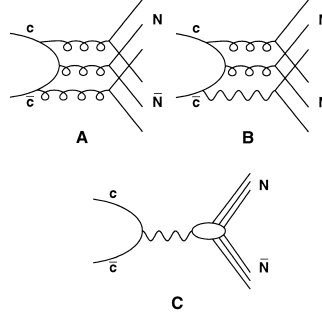


Figure 7: Feynman diagrams of the three main contributions to the J/ψ decay in nucleon-antinucleon. A) purely strong amplitude, B) strong-electromagnetic amplitude and C) purely electromagnetic amplitude. These plots are from reference [34]

rate with high statistical J/ψ sample.

Based on 225M J/ψ events collected at BESIII, the anti-neutron is identified by shower energy deposition and hit information in EMC, with constraints of known center-of-mass energy and back-to-back between neutron and anti-neutron, the branching ratio is determined to be $BR(J/\psi \rightarrow n\bar{n}) = (2.07 \pm 0.01 \pm 0.17) \times 10^{-3}$. At the same time, the branching ratio for $J/\psi \rightarrow p\bar{p}$ is determined to be $BR(J/\psi \rightarrow p\bar{p}) = (2.112 \pm 0.004 \pm 0.027) \times 10^{-3}$. These result improve by a large factor comparing to the previous measurements and strongly support the orthogonal phase of strong and e.m. amplitudes.

2.6 η' and $\eta(1405)$ in $J/\psi \rightarrow \gamma\pi\pi\pi$ decays

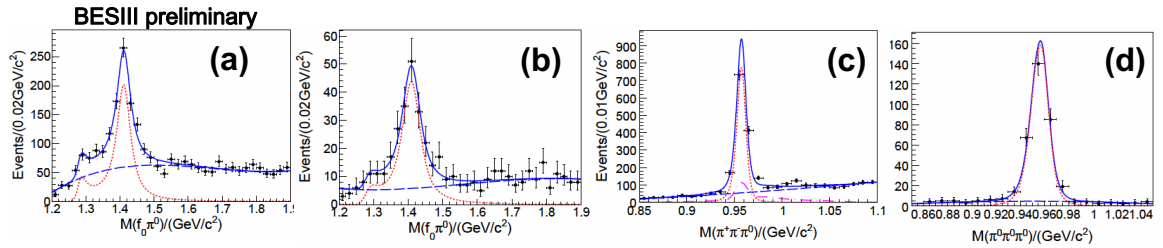


Figure 8: The invariant mass distributions: (a) invariant mass of $f_0(980)\pi^0$ from $J/\psi \rightarrow \gamma\pi^+\pi^-\pi^0$; (b) invariant mass of $f_0(980)\pi^0$ mass from $J/\psi \rightarrow \gamma\pi^0\pi^0\pi^0$; (c) the invariant mass of $\eta' \rightarrow 3\pi$ in $J/\psi \rightarrow \gamma\pi^+\pi^-\pi^0$, (d) mass of $\eta' \rightarrow 3\pi$ from $J/\psi \rightarrow \gamma\pi^0\pi^0\pi^0$, respectively.

The spectrum of radial excitation states of isoscalar η and η' is still not well known. An important issue is about the nature of $\eta(1405)$ and $\eta(1475)$ states, which are not well established. BESIII measured the decays of $J/\psi \rightarrow \gamma\pi^+\pi^-\pi^0$ and $\gamma\pi^0\pi^0\pi^0$. In the two

decay modes, clear $f_0(980)$ signals are observed on both $\pi^+\pi^-$ and $\pi^0\pi^0$ spectra, the width of observed $f_0(980)$ is much narrower (~ 10 MeV) than that in other processes [12]. By taking events in the window of $f_0(980)$ on the $\pi\pi$ mass spectrum, we observed evidence of $f_1(1285)$ in the low mass region of $f_0(980)\pi^0$ as shown in Fig. 8 (a) and (b), which corresponding to significance of about 4.8σ for $f_1(1285) \rightarrow f_0(980)\pi^0$ in $f_0(980) \rightarrow \pi^+\pi^-$ mode (1.4σ in $f_0(980) \rightarrow \pi^0\pi^0$). It is interesting that clear peak around 1400 MeV is also observed on the mass of $f_0(980)\pi^0$ (see Fig. 8 (a) and (b)). Preliminary angular analysis indicates that the peak on 1400 MeV is from $\eta(1405) \rightarrow f_0(980)\pi^0$ decay. BESIII measured the combined branching fraction of $\eta(1405)$ production to be $BR(J/\psi \rightarrow \gamma\eta(1405)) \times BR(\eta(1405) \rightarrow f_0(980)\pi^0) \times BR(f_0(980) \rightarrow \pi^+\pi^-) = (1.48 \pm 0.13 \pm 0.17) \times 10^{-5}$ and $BR(J/\psi \rightarrow \gamma\eta(1405)) \times BR(\eta(1405) \rightarrow f_0(980)\pi^0) \times BR(f_0(980) \rightarrow \pi^0\pi^0) = (6.99 \pm 0.93 \pm 0.95) \times 10^{-6}$, respectively. It is the first time that we observe anomalously large isospin violation in the strong decay of $\eta(1405) \rightarrow f_0(980)\pi^0$.

Following BESIII measurements, in reference [35], the authors interpret this puzzle as an intermediate on-shell $K\bar{K}^* + c.c.$ rescattering to the isospin violating $f_0(980)\pi^0$ by exchanging on-shell kaon. Further experimental study on the $\eta(1405)$ parameters and identification of quantum number are needed at BESIII.

By looking at the invariant mass of $\pi\pi\pi$ in $J/\psi \rightarrow \gamma 3\pi$ decays as shown in Fig. 8 (c) and (d), we observe signals for $\eta' \rightarrow \pi^+\pi^-\pi^0$ and $\pi^0\pi^0\pi^0$ decays, respectively, and determine the decay rates to be $BR(\eta' \rightarrow \pi^+\pi^-\pi^0) = (3.83 \pm 0.15 \pm 0.39) \times 10^{-3}$ and $BR(\eta' \rightarrow \pi^0\pi^0\pi^0) = (3.56 \pm 0.22 \pm 0.34) \times 10^{-3}$, respectively. For $\eta' \rightarrow \pi^+\pi^-\pi^0$ decay, it is consistent with CLEO-c's measurements and precision is improved by a factor of 4. In contrast, for $\eta' \rightarrow \pi^0\pi^0\pi^0$ decay, it is two times larger than that in the PDG value [12].

2.7 Observation of resonances above 2.0 GeV in $J/\psi \rightarrow \gamma\eta'\pi^+\pi^-$ decay

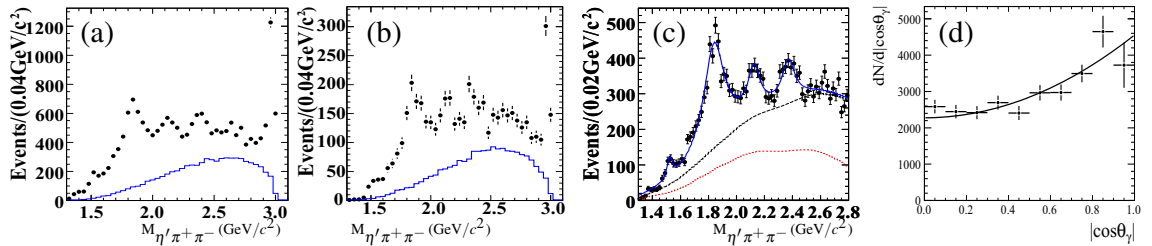


Figure 9: The invariant mass distributions of $\eta'\pi^+\pi^-$ with (a) $\eta' \rightarrow \gamma\rho$ (b) $\eta' \rightarrow \eta\pi^+\pi^-$, and (c) the combined plot for (a) and (b), and fitting results. (d) is for the $\cos\theta_\gamma$ distribution, where θ_γ is the pole angle of the radiative photon. The points with error bar are data. The histograms are from $J/\psi \rightarrow \gamma\eta'\pi^+\pi^-$ phase space MC.

The X(1835) was firstly observed at the BESII with a statistical significance of 7.7σ [36]. The possible interpretations of the X(1835) include a $p\bar{p}$ bound state [37,38], a glueball [39], a

radial excitation of the η' meson [40], etc. We report a study of $J/\psi \rightarrow \gamma \eta' \pi^+ \pi^-$ that used two η' decay modes, $\eta' \rightarrow \gamma \rho$ and $\eta' \rightarrow \pi^+ \pi^- \eta$. Figure 9 (a) and (b) show the $\eta' \pi^+ \pi^-$ invariant mass spectrum in $J/\psi \rightarrow \gamma \eta' \pi^+ \pi^-$ with $\eta' \rightarrow \gamma \rho$ and $\eta' \rightarrow \pi^+ \pi^- \eta$ decay modes, respectively. The $X(1835)$ resonance is clearly seen. Additional peaks are observed around 2.1 and 2.3 GeV/c^2 , denoted as $X(2120)$ and $X(2370)$, as well as the $f_1(1510)$ in the low mass region and the distinct $\eta_c(1S)$ signal in the high mass region.

Fits to the mass spectra have been made using four efficiency-corrected Breit-Wigner functions convolved with a Gaussian mass resolution plus a nonresonant $\pi^+ \pi^- \eta'$ contribution and background representations. The fitting result of the combined mass spectrum is shown in Fig. 9(c). The mass and width of $X(1835)$ are measured to be $M = 1836.5 \pm 3.0^{+5.6}_{-2.1} \text{ MeV}/c^2$ and $\Gamma = 190 \pm 9^{+38}_{-36} \text{ MeV}$ with a significance larger than 20σ . The mass and width for $X(2120)$ ($X(2370)$) is determined to be $M = 2122.4 \pm 6.7^{+4.7}_{-2.7} \text{ MeV}/c^2$ ($M = 2376.3 \pm 8.7^{+3.2}_{-4.3} \text{ MeV}/c^2$) and $\Gamma = 83 \pm 16^{+31}_{-11} \text{ MeV}$ ($\Gamma = 83 \pm 17^{+44}_{-6} \text{ MeV}$) with significance $7.2\sigma(6.4\sigma)$. For $X(1835)$, the $\cos\theta_\gamma$ distribution is shown in Fig. 9, where θ_γ is the polar angle of the radiative photon in the J/ψ center of mass system. It agrees with $(1 + \cos^2\theta_\gamma)$, which is expected for a pseudoscalar.

2.8 Observation of $X(1870) \rightarrow a_0^\pm \pi^\mp$ in $J/\psi \rightarrow \omega \eta \pi^+ \pi^-$ decay

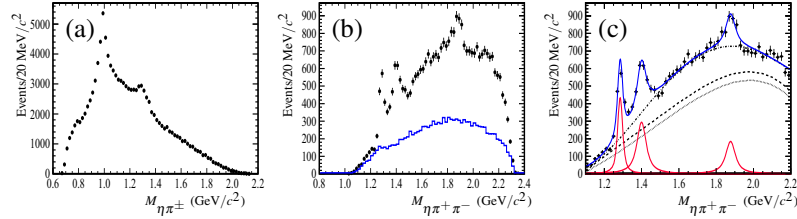


Figure 10: The invariant mass distributions of (a) $\eta \pi^\pm$, (b) $\eta \pi^+ \pi^-$ with events in $a_0(980)$ mass window; (c): fitting results; In (b), the histograms are from $J/\psi \rightarrow \omega \eta \pi^+ \pi^-$ phase space MC.

Experimentally, the study of the production mechanism of the $X(1835)$ and $\eta(1405)$, e.g. searches for them in $\eta \pi \pi$ final states with other accompanying particles (ϕ , ω etc.), are useful for clarifying their nature. In particular, the measurements of the production width of these two states in hadronic decays of the J/ψ and a comparison with corresponding measurements in J/ψ radiative decay would provide important information about the glueball possibility. We present results of a study of $J/\psi \rightarrow \omega \eta \pi^+ \pi^-$, in which the ω decays to $\pi^+ \pi^- \pi^0$ and the η/π^0 decays to a pair of photons. In the mass spectrum of $\eta \pi^p m$, as shown in Fig. 10 (a), the $a_0^\pm(980)$ peak is clearly seen. The mass spectrum of $\eta \pi^+ \pi^-$ with events in the $a_0(980)$ mass window is shown in Fig. 10 (b). Both $f_1(1285)$ and $\eta(1405)$ are observed significantly. A clear peak around 1800 MeV , denoted as $X(1870)$ is also seen for the first time in the decay of $J/\psi \rightarrow \omega \eta \pi^+ \pi^-$. A fit with three resonances with

simple BW formula yields a mass $M = 1877.3 \pm 6.3^{+3.4}_{-7.4}$ MeV/c² and a width $\Gamma = 57 \pm 12^{+19}_{-4}$ MeV for the X(1870) structure with s statistical significance of 7.2σ . Whether the resonant structure of X(1870) is due to the X(1835), the $\eta_2(1870)$, or a new resonance still needs further study such as a partial wave analysis that will be possible with the larger J/ ψ data sample. For the $\eta(1405)$, the product branching ratio of its hadronic production is measured to be smaller than that for its production in the radiative J/ ψ decays [12]. For detail about this analysis, one can find more in reference [41].

2.9 Open charm physics

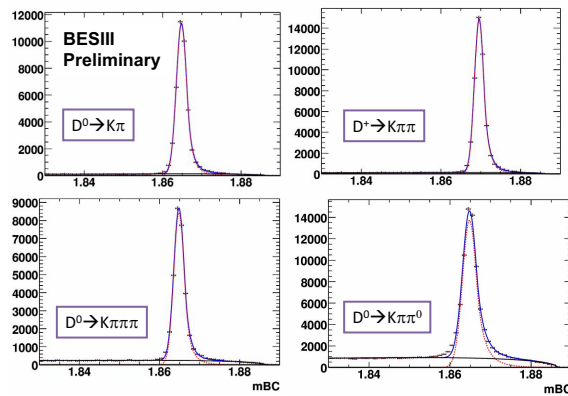


Figure 11: Beam constraint mass distributions.

As of May, 2011, the BESIII has accumulated integrated luminosity of 2.9 fb^{-1} on $\psi(3770)$ peak for open charm physics, which is about 3.5 times the previous largest $\psi(3770)$ data set taken by the CLEO-c Experiment. Taking advantage of the high luminosity provided by the BEPCII collider, BESIII is expected to take much more data at both 3770 MeV and higher energies. Many high precision measurements, including CKM matrix elements related to charm weak decays, decay constants f_D and f_{D^*} , form factors from D semileptonic decays, Dalitz decays, searches for CP violation, and absolute decay branching fractions, will be accomplished in the near future.

There are many advantages of doing charm physics at experiments with e^+e^- collider at threshold. With e^+e^- colliding, the initial energy and quantum numbers are known. For $\psi(3770) \rightarrow D\bar{D}$, both D daughter mesons can be fully reconstructed, allowing absolute measurements, namely, the so called double-tag technique. The continuum background is greatly suppressed by doing this, and kinematic constraints can be applied to infer missing particles on the other side D meson. To demonstrate the cleanliness of the D tags, in Fig. 11, we show a beam-constrained mass plots for some of the fully reconstructed D^0/D^\pm decay modes, from part of data. The beam-constrained mass $m_{BC} = \sqrt{E_{beam}^2 - p_D^2}$, where E_{beam} is the beam energy and p_D is the candidate momentum, is obtained by substituting the

reconstructed D energy with the beam energy. With this technique, the neutrino can be reconstructed in the leptonic and semileptonic D decays, so that decay constants and form factor/CKM matrix elements can be precisely measured. Thus, these precise measurements could be used to test and calibrate the theoretical tools such as lattice QCD, which are critical for dealing with B decays.

3 Summary

The BESIII experiment addresses a wide range of topics in the field of QCD and searches for new physics beyond the standard model. At present the BESIII collaboration has collected a record on statistics on J/ψ , ψ' , and $\psi(3770)$ charmonium states. These data are being exploited to provide precision measurements with a high discovery potential in light hadron and charmonium spectroscopy, charmonium decays, and open charm productions. Most recent highlights from BESIII are reviewed in this paper.

Since very recently, data about 470 pb^{-1} luminosity have been taken at a center-of-mass energy of 4010 GeV, which could give new insights in our understanding of the recently discovered XYZ states and which will allow to explore the field of D_s physics.

Acknowledgements

We would like to thank the accelerator people at BEPCII for their hard work which makes our high luminosity possible. We would also like to thank the great computational and software support of the IHEP staff. This work is supported in part by the Ministry of Science and Technology of China under Contract No. 2009CB825200; 100 Talents Program of CAS.

References

- [1] M. Ablikim *et al.* (BESIII Collaboration), *Design and construction of the BESIII detector*, Nucl. Instrum. Meth. **A614**, 345(2009).
- [2] M. Ablikim *et al.* (BESIII Collaboration), *Measurements of $h_c(1P_1)$ in ψ' Decays*, Phys. Rev. Lett. **104**, 132002 (2010) [hep-ex/1002.0501].
- [3] M. Ablikim *et al.* (BESIII Collaboration), *Evidence for ψ' decays into $\gamma\pi^0$ and $\gamma\eta$* , Phys. Rev. Lett. **105**, 261801 (2010) [hep-ex/1011.0885].
- [4] M. Ablikim *et al.* (BESIII Collaboration), *Branching fraction measurements of χ_{c0} and χ_{c2} to $\pi^0\pi^0$ and $\eta\eta$* , Phys. Rev. D **81**, 052005 (2010) [hep-ex/1001.5360].

- [5] M. Ablikim *et al.* (BESIII Collaboration), *Observation of a $p\bar{p}$ mass threshold enhancement in $\psi' \rightarrow \pi^+\pi^- J/\psi$ ($J/\psi \rightarrow \gamma p\bar{p}$) decay*, Chin. Phys. C **34**, 4 (2010) [hep-ex/1001.5328].
- [6] M. Ablikim *et al.* (BESIII Collaboration), *Confirmation of the X(1835) and observation of the resonances X(2120) and X(2370) in $J/\psi \rightarrow \gamma\pi^+\pi^-\eta'$* , Phys. Rev. Lett. **106**, 072002 (2011) [hep-ex/1012.3510].
- [7] M. Ablikim *et al.* (BESIII Collaboration), *Measurement of the Matrix Element for the Decay $\eta' \rightarrow \eta\pi^+\pi^-$* , Phys. Rev. D **83**, 012003 (2011) [hep-ex/1012.1117].
- [8] M. Ablikim *et al.* (BESIII Collaboration), *First Observation of the Decays $\chi_{cJ} \rightarrow \pi^0\pi^0\pi^0\pi^0$* , Phys. Rev. D **83**, 012006 (2011) [hep-ex/1011.6556].
- [9] M. Ablikim *et al.* (BESIII Collaboration), *Study of $a_0^0(980) - f_0(980)$ mixing*, Phys. Rev. D **83**, 032003 (2011) [hep-ex/1012.5131].
- [10] M. Ablikim *et al.* (BESIII Collaboration), *Study of χ_{cJ} radiative decays into a vector meson*, Phys. Rev. D **83**, 112005 (2011) [hep-ex/1103.5564].
- [11] M. Ablikim *et al.* (BESIII Collaboration), *Observation of χ_{c1} Decays into Vector Meson Pairs $\phi\phi$, $\omega\omega$, and $\omega\phi$* , Phys. Rev. Lett. **107**, 092001 (2011).
- [12] PDG 2010: Particle Data Group, *Review of Particle Physics*, Journal of Physics G **37**, 075021 (2010).
- [13] R. M. Baltrusaitis *et al.* (Mark-III Collaboration), Phys. Rev. D **33**, 629 (1986).
- [14] J. Z. Bai *et al.* (BES Collaboration), Phys. Lett. B **555**, 174 (2003).
- [15] D. M. Asner *et al.* (CLEO Collaboration), Phys. Rev. Lett. **92**, 142001 (2004).
- [16] B. Aubert *et al.* (BABAR Collaboration), Phys. Rev. Lett. **92**, 142002 (2004).
- [17] S. Uehara *et al.* (Belle Collaboration), Eur. Phys. J. C **53**, 1 (2008).
- [18] A. Vinokurova *et al.* (Belle Collaboration), arXiv:1105.0978 [hep-ex].
- [19] R. E. Mitchell *et al.* (CLEO Collaboration), Phys. Rev. Lett. **102**, 011801 (2009).
- [20] V. V. Anashin *et al.* (KEDR Collaboration), arXiv:1012.1694.
- [21] E. Eichten, K. Gottfried, T. Kinoshita, K. D. Lane and T.-M. Yan, Phys. Rev. D **17**, 3090 (1978).
- [22] S.-K. Choi *et al.* (Belle Collaboration), Phys. Rev. Lett. **89**, 102001 (2002).
- [23] D. M. Asner *et al.* (CLEO Collaboration), Phys. Rev. Lett. **92**, 142001 (2004).
- [24] B. Aubert *et al.* (BABAR Collaboration), Phys. Rev. Lett. **92**, 142002 (2004).

- [25] B. Aubert *et al.* (BABAR Collaboration), Phys. Rev. **D 72**, 031101 (2005).
- [26] C. Edwards *et al.* (Crystal Ball Collaboration), Phys. Rev. Lett. **48**, 70 (1982).
- [27] D. Cronin-Hennessy *et al.* (CLEO Collaboration), Phys. Rev. **D 81**, 052002 (2010).
- [28] B. Aubert *et al.* (Babar Collaboration), Phys. Rev. **D 78**, 012006 (2008).
- [29] L. L. Wang, for the BESIII Collaboration, this conference (preliminary results).
- [30] A. Vinokurova *et al.* (Belle Collaboration), arXiv:1105.0978.
- [31] P. del Amo Sanchez *et al.* (BABAR Collaboration), Phys. Rev. **D 84**, 012004 (2011).
- [32] T. K. Pedlar *et al.* (CLEO Collaboration), Phys. Rev. **D 79**, 111101 (2009).
- [33] Q. Zhao, Phys. Lett. **B697**, 52(2011).
- [34] R. Baldini *et al.* (FENICE Collaboration), Phys. Lett. **B 444**, 111 (1998).
- [35] J.-J. Wu, X.-H. Liu, Q. Zhao and B.-S. Zou, arXiv: 1108.3772.
- [36] M. Ablikim *et al.* (BESII Collaboration) Phys. Rev. Lett. **95**, 262001 (2005).
- [37] G. J. Ding and M. L. Yan, Phys. Rev. **C 72**, 015208 (2005).
- [38] G. J. Ding and M. L. Yan, Eur. Phys. J. **A 28**, 351 (2006).
- [39] B. A. Li, Phys. Rev. **D 74**, 034019 (2006).
- [40] T. Huang and S. L. Zhu, Phys. Rev. **D 73**, 014023 (2006).
- [41] M. Ablikim *et al.* (BESIII Collaboration), arXiv:1107.1806.